Calculations of Site-Specific CO Stretching Frequencies for Copper Carbonyls with the "Near Spectroscopic Accuracy": CO Interaction with Cu^+/MFI

Ota Bludský, Martin Šilhan, Dana Nachtigallová, and Petr Nachtigall*

J. Heyrovský Institute of Physical Chemistry, Academy of Sciences of the Czech Republic and Center for Complex Molecular Systems and Biomolecules, Dolejškova 3, 182 23, Prague 8, Czech Republic

Received: August 22, 2003; In Final Form: September 22, 2003

A scaling method based on the linear correlation between the CO bond length and the CO stretching frequency has been applied to the CO molecule adsorbed on the Cu-exchanged MFI zeolite. Effects of anharmonicity, cluster size, unit cell size, and the Madelung potential were investigated. Interaction of CO with zeolite framework was described at the combined RI−BLYP/IPF level. The inner part of the combined model (RI−BLYP description) consisted of up to 23 TO_4 tetrahedra. The effect of the Madelung potential on CO stretching frequencies was negligible. All Cu^+ sites on the channel intersection and on the wall of the main channel are characterized by the CO stretching frequencies in the narrow range of 2159−2164 cm^{-1} in excellent agreement with experimental data. The Cu^+ sites on the wall of the zigzag channel show slightly higher frequencies (3−6 cm^{-1}). These sites are populated, however, only when the framework Al atoms are at T4 or T10 positions. The proposed computational scheme provides essentially the same level of accuracy as obtained from CCSD(T) calculations for small copper carbonyl species with overall error smaller than 5 cm^{-1}.

1. Introduction

Transition-metal carbonyls have been the subject of numerous theoretical and experimental studies because of their importance in modern coordination chemistry, organometallic chemistry, and catalysis.[1,2] The large effort was directed toward characterization of active sites in zeolites and other molecular environments using carbon monoxide as a probe molecule. It was shown that the CO stretching frequency is very sensitive to the interaction of the transition metal with surrounding environment that controls catalytic properties of the active site.[3−16] Interpretation of the experimental infrared spectra of transition-metal carbonyl species (M−CO) has become an invaluable tool in understanding the structure and properties of catalytically active sites and has received considerable attention from theoretical chemists over the past decade. The nature of the C−O bond is usually described in terms of M←CO σ-donation and M→CO π-back-donation effects. The σ-donation tends to increase the M−CO bonding and, therefore, it increases the CO stretching frequency, while the π-back-donation decreases the bonding and lowers the frequency.[17,18]

Monocarbonyl Cu^+ complexes formed by adsorption of CO on Cu-exchanged zeolites are among the most extensively studied copper carbonyl species because of high catalytic activity of the Cu/zeolite system for decomposition of NO to molecular nitrogen and oxygen.[19] IR bands in the range of 2108−2160 cm^{-1} were assigned to the CO stretching mode of monocarbonyls in Cu^+/zeolite systems.[20] Thus, the CO stretching frequency is either red shifted or blue shifted with respect to the gaseous CO (2143 cm^{-1}). Theoretical approaches employed in rationalization of experimental data range from the simplest models providing general insight only to elaborate models of the zeolite framework.[21−25] Theoretical models of CO/Cu^+/MFI often fail to reproduce experimentally observed blue shift of CO stretching mode. Ramprasad et al. used water ligands to represent the zeolite-framework oxygen atoms coordinated directly to the Cu^+ ion.[21] Although their model neglects some important features of the zeolite environment such as the topology of the zeolite structure, the local zeolite charges induced by the Si/Al substitution, and the long-range electrostatic field of zeolite, a clear linear correlation between the CO bond length and the CO stretching frequency was firmly established. However, the blue shift found with this simple model is probably a consequence of fortuitous cancellation of error because of the used model and DFT method. Various models of CO/Cu^+/MFI system containing at least one AlO_4 tetrahedron (and 0−6 SiO_4 tetrahedra) were used together with DFT methods. None of these models was able to reproduce experimentally observed blue shift in the CO stretching mode. Treesukol et al. used the electrostatic embedding method (SCREEP) to include the long-range electrostatic interactions in the CO/Cu/zeolite system.[22] They found that inclusion of the Madelung potential is necessary for correct description of the blue shift of the CO stretching vibration in copper-exchanged zeolites. However, this conclusion was questioned by Davidová et al., who suggested that the description of CO stretching vibration in Cu^+ carbonyl at the DFT level results in qualitatively incorrect red shift.[23] All previously used approaches have obvious drawbacks: insufficient treatment of the electron correlation, neglecting the anharmonic effects, and relatively small models representing the zeolite framework; therefore, the calculated CO stretching frequencies cannot be directly compared with experiment.

Recently, we reported an ab initio study of the Cu^+CO ion that belongs to the class of "nonclassical" transition-metal carbonyls characterized by the CO stretching frequency blue shifted from the gas-phase CO.[26] Comparison of the results obtained using the second-order Moller−Plesset (MP2) and density functional theory (DFT) methods with the more accurate coupled-cluster (CCSD(T)) calculations showed that any com-

* Address correspondence to this author. E-mail: petr.nachtigall@jh-inst.cas.cz.

10.1021/jp036504b CCC: $25.00
Published on Web 10/31/2003

putational approach tractable for the Cu/zeolite system has at best an accuracy of tens of wavenumbers.

Conventional quantum chemistry methods overestimate or underestimate the observed vibrational frequencies in a systematic manner and, therefore, introduction of scaling factors is commonly used for comparison with experiment. Scaling of ab initio harmonic frequencies to experimental fundamentals is certainly very helpful for large systems.[27−29] However, for the precise calculations of frequency shifts due to the interaction with environment, the error bars obtained by this approximation are often unacceptably large. In this paper, we present a novel scaling method based on the linear correlation between the CO bond length and the CO stretching frequency. Contrary to the standard scaling approach where the scaling factors are obtained by comparison of calculated frequencies to a small set of unambiguously assigned fundamentals, our method relies on comparison of DFT frequencies to theoretical benchmark calculations performed at the CCSD(T) level with a large basis set. Moreover, the CCSD(T)/DFT scaling is highly selective since the scaling factor depends on the CO bond distance. We believe that our approach can be used for reliable predictions of the CO stretching frequency in copper carbonyls with near spectroscopic accuracy (to within 5 cm^{-1}). The applicability of the proposed method is demonstrated on the CO/Cu/zeolite system.

Computational details are described in Section 2, results are presented in Section 3, discussion is given in Section 4, and conclusions are drawn in Section 5.

2. Calculations

X_n...Cu^+CO Models. The equilibrium structures and vibrational frequencies of Cu^+CO and model systems ($L-Cu^+CO$, $L = H_2O$, $(H_2O)_2$, OH^-, F^-, and $(F^-)_2$) were calculated at the CCSD(T),[30,31] MP2, and DFT (employing the BLYP and B3LYP exchange correlation functionals[32−35]) levels. The most reliable CCSD(T) calculations were carried out with the effective-core relativistic pseudopotential (replacing 10 inner electrons) and valence (8s7p6d2f1g)/[6s5p3d2f1g] basis sets, denoted ECP-2f1g, for Cu atom[36−38] and correlation consistent valence-quadruple-ζ basis set with polarization functions, cc-pVQZ, for C, O, F, and H atoms[39,40] (this combination of basis sets will be denoted as "Basis set 1", BS1). The DFT and MP2 calculations were carried out with valence-triple-ζ basis set with polarization functions, VTZP, for C, O, and F atoms and valence-triple-ζ basis set for Cu and H ("Basis set 2", BS2).[41,42]

Zeolite/Cu^+CO. The structures of CO molecules adsorbed on the Cu^+ sites in MFI were obtained by energy minimization using the QM-Pot method.[43] Within this approach, the system is divided into two parts: (i) the inner part described at more sophisticated level of theory and (ii) the outer part described at computationally less expensive level. Periodic boundary conditions were applied to the unit cell consisting of 192 T-atoms (191 Si atoms and 1 Al atom) and 384 O atoms. Some calculations were performed with the unit cell of half this size. The inner part of the QM-Pot model consisted of CO molecule, Cu atom, AlO_4 tetrahedron, and a number of framework SiO_4 tetrahedra. The OH saturation of atoms on the boundary of the inner part was always used. The size of the inner part depended on the particular framework Al atom position and on the Cu^+ site: the interaction of Cu^+ ion with framework and CO interaction with Cu^+ and with the framework was described at the DFT level. The clusters (inner part and cluster-terminating H atoms) were described with the BS2 basis set and either with B3LYP hybrid density functional (the cluster-size effect and Madelung potential investigation) or with BLYP exchange-correlation functional (MFI/Cu^+CO investigation), employing the resolution of identity (RI) approximation.[44,45] The (17s4p4d3f4g)/[7s4p2d3f2g], (12s6p5d1f1g)/[5s3p2d1f1g], (12s4p5d1f)/[5s3p2d1f], (9s3p3d1f)/[7s3p3d1f], (9s3p3d1f)/[7s3p3d1f], (4s2p1d)/[3s2p1d] auxiliary basis sets[46−48] were used in RI calculations for Cu, Si, Al, C, O, and H atoms, respectively. The interactions between atoms outside the inner part (outer part) and cross-interactions between atoms from the inner and outer parts were treated at the interatomic potential function (IPF) level, employing the core−shell model potentials developed previously.[49,50] The calculations were carried out with the QM-Pot program[43] which makes use of the TurboDFT[44] and GULP[51] programs for DFT and IPF calculations, respectively. Calculations at the CCSD(T) and MP2 levels were pefromed with the Molpro program suite.[52−54]

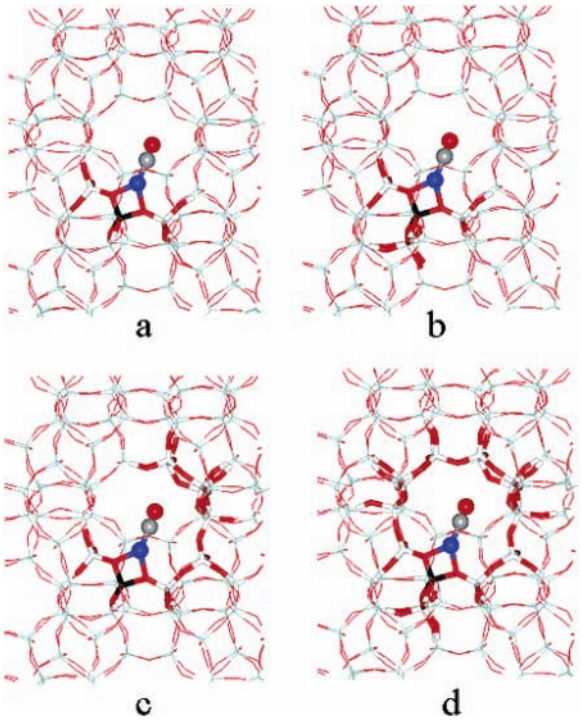

Figure 1. Combined quantum mechanical/interatomic potential function models used in this work viewed along the direction of the zigzag channel: 3-T model (a), 5-T_d model (b), 9-T model (c), and 16-T_d model (d). Cu atom and CO molecule are depicted as circles, atoms of the inner part of the model are depicted in the tube mode, and atoms of the outer part are depicted in the wire mode. Aluminum atom is black and oxygen atoms are red. Framework aluminum atom is located in T12 position, the Cu^+ ion is in I2 site located on the intersection of two channels (type II site).

Calculations of the site-specific CO stretching frequencies were carried out for 12 distinguishable framework Al positions within the orthorhombic symmetry (numbering scheme from ref 55). The CO interaction with the Cu^+ site with the minimum energy for a particular framework Al position was investigated. Depending on the framework Al atom position, the Cu^+ ion coordinates either in type I site on top of the six-membered ring on the wall of one of the channels (Z6, M7, or M6 sites) or in type II site located on the channel intersection (I2 site). For details on Cu^+ coordination in MFI see refs 50 and 23.

The cluster-size effect on the CO stretching vibration was investigated at the QM-Pot level with the inner part described with 3-T ($COCu^+AlSi_2O_{10}H_8$), 5-T_d ($COCu^+AlSi_4O_{16}H_{12}$), 9-T ($COCu^+AlSi_8O_{27}H_{18}$), and 16-T_d ($COCu^+AlSi_{15}O_{45}H_{26}$) clusters (see Figure 1 for details). In addition, the results for 0-T model

TABLE 1: Equilibrium CO Distances (Å) and Harmonic Frequencies (cm^{-1}) Calculated at the CCSD(T), DFT, and MP2 Levels

	CCSD(T)/BS1[a]		B3LYP/BS2[a]		BLYP/BS2[a]		MP2/BS2[a]	
	r_{CO}	ω_{CO}[b]	r_{CO}	ω_{CO}	r_{CO}	ω_{CO}	r_{CO}	ω_{CO}
CO	1.1314	2164.4	1.1268	2219.5	1.1389	2118.1	1.1387	2131.2
Cu^+CO	1.1197	2273.7	1.1167	2314.3	1.1313	2194.7	1.1304	2190.3
$H_2O...Cu^+CO$	1.1219	2257.5[c]	1.1188	2297.5	1.1339	2178.2	1.1321	2179.7
$(H_2O)_2...Cu^+CO$	1.1258	2228.6[c]	1.1233	2258.8	1.1390	2140.5	1.1365	2139.2
$F^-...Cu^+CO$	1.1322	2185.9	1.1292	2222.5	1.1466	2100.2	1.1424	2106.5
$HO^-...Cu^+CO$[d]	1.1352	2168.0	1.1317	2200.8	1.1498	2076.3	1.1453	2083.8
$(F^-)_2...Cu^+CO$	1.1539	2055.6	1.1484	2085.0	1.1682	1963.7	1.1682	1978.8

[a] Basis sets defined in Section 2. [b] Obtained from 2D (Cu−C,C−O) grid. [c] H_2O geometry was taken from B3LYP/BS2 calculation. [d] Linear structure.

(only Cu^+CO treated at the DFT level) are also reported. The effect of the long-range Coulomb interaction of CO with the framework atoms outside of the inner part was also investigated. Calculations with no charge on C and O atoms of CO ("noQ" model) as well as the calculations with charges $q_C = 0.3656$ and $q_O = -0.3656$ were carried out. This charge was determined from natural bond orbital analysis of 3-T cluster model. At the B3LYP/BS2 level, the charges on C and O atoms are 0.3320 and −0.3992. These values were shifted by +0.0336 to satisfy the zero-charge transfer between the Cu^+ and CO fragments and thus avoiding the reparametrization of $Cu^+...Z$ interaction potentials that were obtained for Cu^+ with formal charge +1.

Vibrational Calculations. The CO stretching frequencies for all studied copper carbonyl species were calculated using the two-dimensional (Cu−C,C−O) stretching Hamiltonian (see ref 26). The matrix elements were evaluated on a grid of 7 × 5 points (7 grid points for the C−O coordinate) generated by the corresponding harmonic wave functions. Numerical stability of the Gauss−Hermite quadrature with respect to the grid size was checked on a larger grid (9 × 9 points) for the bare Cu^+CO ion. Three-dimensional anharmonic calculations were performed for $X...Cu^+CO$ systems on a grid of 7 × 5 × 5 points (C−O, Cu−C, X−Cu) and on a grid of 7 × 5 × 5 points (C−O, Cu−C, and Cu−C−O angle) for ZCu^+CO.

3. Results

The computational scheme suggested previously[26] for assessment of reliable vibrational frequencies of transition-metal ion (TMI) carbonyls interacting with molecular environment consists of the following steps: (i) precise calculations of harmonic frequencies for the gas-phase ion using high level ab initio calculations, (ii) treatment of anharmonic effects, and (iii) calculation of frequency shifts due to the interaction of a bare ion with molecular environment. Computational step (i) requires highly accurate treatment of the electron correlation, typically at the CCSD(T) level of theory, steps (ii) and (iii) are usually less demanding and, therefore, lower level ab initio methods as MP2 or DFT can be employed to fulfill the same accuracy goal. The proposed scheme was successfully applied to TMI carbonyls trapped in rare gas matrixes. For example of Cu^+CO and Ag^+CO in Ne and Ar matrixes, the CO stretching frequency can be calculated with near spectroscopic accuracy (to within 5 cm^{-1}).[26,56]

In this study, we focus on a more complicated case of TMI carbonyls in molecular sieves. While the CO frequency shift in Ne matrix was rather small (9 and 3 cm^{-1} for Cu^+CO and Ag^+CO, respectively), the CO frequency shift in Cu^+/MFI system is as large as 86 cm^{-1} (2243 and 2157 cm^{-1} for gas-phase Cu^+CO and in MFI, respectively). Thus, the error introduced by ab initio methods used for the calculations of the frequency shifts due to the effect of the interaction with the environment (MP2 or DFT) is definitely greater than 5 cm^{-1}. To solve this problem, we propose a method for CCSD(T)/DFT scaling of the CO stretching frequency on the basis of the $\omega_{CO}-r_{CO}$ correlation. Scaling was carried out on a series of small models ($L-Cu^+CO$, L = H_2O, $(H_2O)_2$, OH^-, F^-, and $(F^-)_2$) and it was subsequently used in the study of CO/Cu^+/MFI. In this approach, the effect of the Cu^+CO ion interaction with its environment is thus reduced to the proper description of the changes of CO bond length. The quality of the used model for description of the effect of the zeolite environment was also investigated; the following effects were tested: the effect of the inner part used in the combined QM-Pot model, the effect of the unit cell size, and the effect of the Madelung potential.

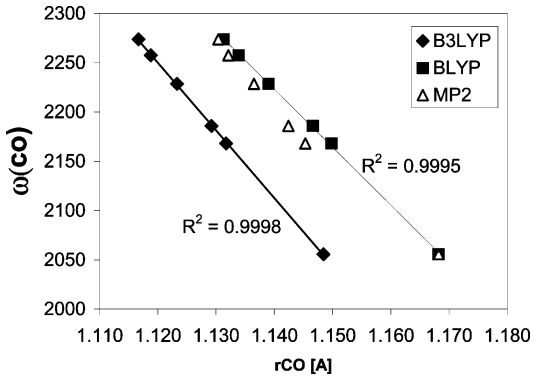

Figure 2. $\omega_{CO}-r_{CO}$ correlation between the CO stretching frequency (in cm^{-1}) calculated for small molecules ($L-Cu^+CO$, L = H_2O, $(H_2O)_2$, OH^-, F^-, and $(F^-)_2$) at the CCSD(T)/BS1 level and CO bond length (in Å) calculated at the B3LYP, BLYP, and MP2 levels.

3.1. $X_n...Cu^+CO$ Models. Equilibrium CO distances and harmonic frequencies calculated at the CCSD(T), DFT, and MP2 levels of theory for a set of small molecules containing the Cu^+CO ion are summarized in Table 1. The molecules were selected to cover a wide frequency range, spanning over 200 cm^{-1}. The CCSD(T) harmonic frequencies were obtained from the two-dimensional (2D) (Cu−C, C−O) grid. Reduction of vibrational problem to two dimensions, however, leads to only very small error on the CO stretching frequency. For the FCuCO molecule, the difference between the full-dimensional analytical CO frequency obtained at the B3LYP level and the corresponding value obtained from the 2D grid is about 0.05 cm^{-1}. A somewhat larger error of 0.12 cm^{-1} was found for $(H_2O)_2...Cu^+CO$.

A brief inspection of Table 1 reveals linear correlation between the CO frequency, ω_{CO}, and the CO distance, r_{CO}. The correlation is shown in Figure 2, where the CCSD(T) frequencies are plotted against r_{CO} calculated at the DFT and MP2 levels. The standard error of estimate is 1.34 and 1.90 cm^{-1} for B3LYP and BLYP functionals, respectively. The standard error for MP2 is much larger (9.6 cm^{-1}). Obviously, the correlation can be used for obtaining highly accurate estimates of ω_{CO}

(essentially with CCSD(T) accuracy) from geometry optimization at the DFT level of theory. Using the ab initio data from Table 1, the following prescriptions for evaluating the CO harmonic frequencies were obtained

$$\omega_{CO}[\text{CCSD(T), cm}^{-1}] = -6875\, r_{CO}[\text{B3LYP, Å}] + 9950 + \Delta\omega_{CO}[\text{CCSD(T), cm}^{-1}] \quad (1)$$

and

$$\omega_{CO}[\text{CCSD(T), cm}^{-1}] = -5878\, r_{CO}[\text{BLYP, Å}] + 8924 + \Delta\omega_{CO}[\text{CCSD(T), cm}^{-1}], \quad (2)$$

where the error of the $\omega_{CO}-r_{CO}$ correlation, $\Delta\omega_{CO}$, is the difference between the calculated (numerically exact CCSD(T) harmonic frequency) and scaled CCSD(T)/DFT harmonic frequencies. The coefficients in eqs 1 and 2 are basis set dependent and, therefore, they can be only used with BS2 basis employed in the DFT calculations in this work.

For most copper carbonyl species, $\Delta\omega_{CO}$ is expected to be rather small (typically less than 5 cm^{-1}) and can be estimated at the DFT level of theory

$$\Delta\omega_{CO}[\text{CCSD(T), cm}^{-1}] \approx \Delta\omega_{CO}[\text{DFT, cm}^{-1}] \quad (3)$$

The $\Delta\omega_{CO}$[DFT] are deviations of the DFT harmonic frequencies from the $\omega_{CO}-r_{CO}$ correlation calculated at the DFT level with coefficients (−7186, 10336) and (−6231, 9242) for the B3LYP and BLYP functionals, respectively.

3.2. Anharmonic CO Frequencies. To investigate the effect of anharmonicity on the CO stretching frequency, we carried out vibrational calculations on the two- and three-dimensional grids (see Section 2) for several copper carbonyl species. All anharmonic calculations were performed at the DFT level using the B3LYP and BLYP functionals. For the gaseous Cu^+CO ion, B3LYP/BS2 overestimates the CO harmonic frequency by 42 cm^{-1}. The corresponding anharmonic correction (−24.8 cm^{-1}), however, is fairly close to the CCSD(T)/BS1 value (−25.5 cm^{-1}). We expect similar behavior for other copper carbonyl species. The B3LYP/BS2 anharmonic corrections are −24.0, −23.6, −23.8, −24.1, and −24.6 cm^{-1} for $H_2O...Cu^+CO$, $(H_2O)_2...Cu^+CO$, $F^-...Cu^+CO$, $OH^-...Cu^+CO$, and $(F^-)_2...Cu^+CO$, respectively. As expected, the CO vibration does not couple with vibrations beyond the heavy copper atom even if anharmonic contributions are taken into account. For FCuCO, the CO stretching frequencies calculated from the 2D (Cu−C, C−O) and 3D (F−Cu, Cu−C, C−O) grid differ only by 0.3 cm^{-1}. Therefore, the largest anharmonic effect for copper carbonyl species is coupling with the Cu−C−O bending vibration. Neglecting the bending mode in the 2D stretching model increases the CO stretching frequency by 3.4 cm^{-1}. Comparison of the CO frequencies obtained from the two-dimensional grid led us to conclude that the anharmonic effect on the CO stretching frequency is about the same for all studied systems. Thus, throughout this study we used the CCSD(T) anharmonic correction of −29 cm^{-1} calculated on 3D grid (Cu−C, C−O, and Cu−C−O angle) previously for the gas-phase Cu^+CO ion as our best estimate.[26]

3.3. Effect of the Madelung Potential and the Cluster-Size Effect. The cluster-size effect was studied within the embedding scheme employing clusters of sizes 0-T, 3-T, 5-T_d, 9-T, and 16-T_d (for details see Section 2 and Figure 1) of the Cu^+ I2 site with framework Al atom at T12 position. The geometry optimization was carried out with zero charge on C and O atoms (no effect of the Madelung potential generated by the lattice atom outside the inner part of the model) and with NBO charges on C and O atoms (see Section 2). The latter model accounts for the Madelung potential effect at the molecular mechanics level (point charge interaction), however, the wave function is not perturbed by the Madelung potential generated by the atoms outside the inner part of the model. The resulting Cu−C and C−O distances and harmonic CO stretching frequencies ω_{CO}[CCSD(T)] calculated according to eq 1 are summarized in Table 2.

TABLE 2: Calculated Cu−C and C−O Bond Lengths (in Å) and Harmonic CO Stretching Frequencies (in cm^{-1}) Obtained with Various Definition of the Inner Part of Embedding Scheme for CO on Cu^+ at I2 Site with Al Atom at T12 Position[d]

model[a]	r(Cu−C)[b]	r(C−O)[b]	harmonic[c]
0T-noQ	1.8945	1.1170	2266.6
3T-noQ	1.8085	1.1321	2162.8
5T_d-noQ	1.8097	1.1315	2166.9
9T-noQ	1.8167	1.1287	2186.2
16T_d-noQ	1.8189	1.1285	2187.4
0T	1.8831	1.1195	2249.4
3T	1.8166	1.1318	2164.9
5T_d	1.8180	1.1312	2169.0
9T	1.8211	1.1289	2184.8
16T_d	1.8180	1.1284	2188.0

[a] The size of the inner part of the QM-Pot model. [b] Geometry optimized at the QM-pot level employing B3LYP/BS2 for the description of the inner part of combined model. [c] Harmonic frequencies evaluted according to eq 1. [d] Results of calculations with no charges on CO (denoted "-noQ") and with NBO charges are reported.

First, we discuss the effect of the cluster size without the Madelung potential. Within the 0-T model, the CuCO species carries a positive charge +1.00 while this charge is reduced in other models because of the charge transfer between the copper and zeolite framework.[57] Consequently, the CO stretching frequency calculated with 0-T model is significantly overestimated. The CO stretching frequency calculated with 3-T and 5-T_d models are more than 20 cm^{-1} smaller than those calculated with larger 9-T and 16-T_d models. In the latter models, the CO interaction with the zeolite framework atoms on the opposite site of the channel is treated at the DFT level while this interaction is described only at the IPF level with smaller cluster models (see Figure 1). Obviously, the proper description of the CO interaction with framework atoms from the opposite side of the channel is critical for precise description of CO stretching dynamics.

As can be seen from Table 2, the results obtained with and without charges on CO are very similar. Inclusion of the electrostatic potential increases the CO stretching frequency by 2−3 cm^{-1} for the small QM model and is negligible for larger models (<1 cm^{-1}). Calculations with the unit cells containing 96 and 192 T-atoms (Si or Al) show that the effect of the unit-cell size is rather marginal (−0.7 cm^{-1}).

The Madelung potential description given above (mechanical embedding) does not account for the wave function perturbation due to the potential. Recently, Treesukol et al. concluded that the blue shift in CO stretching frequencies is due to the Madelung potential effect on the electronic wave function.[22] They used a SCREEP method within which the electrostatic potential of the crystal lattice is represented by a finite number of point charges located on a surface enclosing the QM cluster. While for the systems not requiring the use of the link atom this model is certainly very useful, the effect of the cluster-terminating H atoms used in zeolite models is, however, unclear and it is a possible source of an error of this model. To avoid

possible problems connected to link atoms, we have modified the method for description of the electrostatic embedding in the following way: The electrostatic potential of the outer part was evaluated on the surface enclosing the bare Cu^+CO ion only. This potential was constructed as the difference of the electrostatic potential of the whole lattice and electrostatic potential of the inner-part atoms, including the link atoms. The potential was evaluated on the surface constructed from spheres around Cu, C, and O atoms with the radius of 1.8 times van der Waals radius. The Madelung potential effect was then calculated as the change of the CO stretching frequencies of Cu^+CO calculated with and without the potential. The calculations performed with 3-T and 16-T_d embedded models gave $\Delta\omega_{CO}^{Madelung}$ of +3.2 and +0.9 cm^{-1}. To verify that the choice of the Cu^+CO geometry is not critical for this model, $\Delta\omega_{CO}^{Madelung}$ was also calculated with geometries taken from the gas-phase Cu^+CO and potential generated from 3-T and 16-T_d embedding model. Resulting $\Delta\omega_{CO}^{Madelung}$ of +2.5 and +0.3 cm^{-1} for 3-T and 16-T_d models, respectively, are close to those obtained with geometries taken from the energy minimization with 3-T and 16-T_d embedding models. Thus, we conclude that the effect of the Madelung potential on the wave function is small and that this effect decreases with the increasing size of the inner part.

3.4. Vibrational Frequencies of CO Adsorbed on Cu^+/MFI. Adsorption of CO on twelve Cu^+ sites in MFI was investigated. Framework Al atom was placed to one of the twelve distinguishable T-positions (assuming orthorhombic symmetry[55]) and Cu^+ ion was placed in the most stable site for each of the framework Al atom positions.[50] The geometry of the system was optimized at the RI−BLYP/BS2 level using the combined QM-Pot model, and the CO stretching frequencies were calculated according to eq 2 with $\Delta\omega_{CO} \approx -4$ cm^{-1} and $\Delta\nu \approx -29$ cm^{-1}. The $\Delta\omega_{CO}$ correction was obtained for I2 site with framework atom in T12 position and 16-T_d size of the inner part of the model and it was used for all sites considered in this study.

Two definitions of inner part were used: (i) the minimum size model for the description of the Cu^+ interaction with the framework and (ii) the large inner part model in which framework atoms close to CO are also included. The former definition requires 3-T model for Cu^+ sites on the intersection (type II sites) and 6-T_r cluster models (6 TO_4 tetrahedra in the six-membered ring) for Cu^+ sites on the channel wall (type I sites), with the exception of M7 site which requires 7-T model (see ref 50 for details). The latter model requires the use of the inner part consisting of 12−23 framework TO_4 tetrahedra. The model size depends on the location of the carbonyl in the channel system of MFI. The 16-T_d model for framework Al atom at T12 site is depicted in Figure 1d.

Optimized C−O bond lengths and calculated CO stretching vibrations ν_{CO} obtained with both models are summarized in Table 3. The increase of the model size results in the increase of the CO stretching vibrations by almost the constant factor of 20 cm^{-1}. The results in Table 3 are ordered according to the increasing CO stretching frequency obtained with the large model. All calculated frequencies are in the range of 11 cm^{-1}. All Cu^+ sites on the channel intersection (I2 sites) and on the wall of the main channel (M6 and M7 sites) are characterized by the CO stretching frequencies in the narrow range of 2159−2164 cm^{-1}. Only the Cu^+ sites on the wall of the zigzag channel (Z6 sites) show slightly higher frequencies (increase of 3−6 cm^{-1}); however, these sites are populated only when framework Al atom is at the T4 or T10 positions.

TABLE 3: RI−BLYP CO Distances [Å] and the Scaled CCSD(T) CO Stretching Frequencies [cm^{-1}] Calculated at Various MFI Sites with Small and Large Definition of Inner Part of Embedding Model

MFI site/ Al position[a]	small inner part definition			large inner part definition		
	model[b]	r_{CO}	ν_{CO}	model[b]	r_{CO}	ν_{CO}
M6/T11	3T	1.1477	2145	14T	1.1453	2159
I2/T12	3T	1.1491	2136	16T	1.1453	2159
I2/T5	3T	1.1482	2141	12T	1.1451	2160
I2/T2	3T	1.1485	2140	12T	1.1450	2161
I2/T1	7T	1.1482	2142	23T	1.1449	2161
I2/T3	3T	1.1482	2141	13T	1.1448	2162
M6/T8	6T	1.1474	2147	22T	1.1447	2162
I2/T9	3T	1.1476	2145	13T	1.1446	2163
I2/T6	3T	1.1478	2144	12T	1.1444	2164
M7/T7	3T	1.1484	2140	17T	1.1444	2164
Z6/T4	6T	1.1476	2145	21T	1.1439	2167
Z6/T10	6T	1.1455	2158	18T	1.1434	2170

[a] Cu^+ site in MFI before interaction with CO molecule. Classification according to ref 50 adopted. [b] Number of framework T-atoms in the inner part of the QM-Pot model treated at the DFT level.

3.5. CCSD(T)/DFT Scaling. Reliability of the proposed computational scheme was tested on small molecules for which the CCSD(T) calculation is feasible. The major source of error is, of course, the difference between the calculated and scaled CCSD(T) harmonic frequencies, $\Delta\omega_{CO}$, and its approximation at the DFT level of theory (see eq 3). Even if $\Delta\omega_{CO}$ was reduced below 5 cm^{-1} for most studied systems by employing the CCSD(T)/DFT scaling on the basis of the $\omega_{CO}-r_{CO}$ correlation, validity of eq 3 remains to be checked. Therefore, we carried out CCSD(T), B3LYP, and BLYP calculations for the $Cl^-...Cu^+CO$ molecule where the largest deviation from the $\omega_{CO}-r_{CO}$ linear dependence was found. Assuming anharmonicity of 29 cm^{-1}, the CCSD(T) prediction of the CO stretching frequency, 2159 cm^{-1}, is in very good agreement with experimentally determined value of 2156.5 cm^{-1}.[58] At the DFT level, the CO distances 1.1277 Å (B3LYP) and 1.1444 Å (BLYP) correspond to the scaled CO frequency of 2168 cm^{-1}. Thus, the CCSD(T)/DFT scaling overestimates the CO frequency by 9 cm^{-1}. Apparently, the basis set used for the third row elements is not fully consistent with respect to the $\omega_{CO}-r_{CO}$ correlation in Figure 2. As suggested in Section 3, the $\Delta\omega_{CO}$ correction can be estimated from $\omega_{CO}-r_{CO}$ calculated at the DFT level of theory. For $Cl^-...Cu^+CO$, the corresponding $\Delta\omega_{CO}$ estimates are −8 cm^{-1} and −7 cm^{-1} at the B3LYP and BLYP levels, respectively. When the $\Delta\omega_{CO}$ correction is used, the CO stretching frequencies are overestimated by only 1 and 2 cm^{-1} at the B3LYP and BLYP levels, respectively. Similar results were obtained for the Cu^+/MFI system. The $\Delta\omega_{CO}$ values are, however, much smaller. For the 16-T_d model of the I2/T12 site, both functionals give the same $\Delta\omega_{CO}$ of −4 cm^{-1}. The remaining error in the CCSD(T) harmonic frequency, ω_{CO}, should not exceed the standard error of estimate of the $\omega_{CO}-r_{CO}$ correlation in Figure 2 (less than 2 cm^{-1}). We conclude that the CCSD(T)/DFT scaling of ω_{CO} on the basis of the $\omega_{CO}-r_{CO}$ correlation provides essentially the same level of accuracy as obtained from the CCSD(T) calculations.

4. Discussion

The majority of theoretical studies failed to reproduce a blue shift upon the adsorption of CO molecule on Cu^+/MFI (except for poor models where the zeolite framework is represented by few water molecules).[21,23,24] When the model representing the zeolite framework contains aluminum atom, the CO stretching

TABLE 4: B3LYP and Scaled CCSD(T) CO Stretching Frequencies ν_{CO} (in cm^{-1}) Calculated for Gas-Phase CO and CO/Cu$^+$/MFI (I2 site with Al at T$_{12}$) with Various Models[a]

	B3LYP		scaled CCSD(T)	
$(CO)_g$	2192	[+49]	2138[b]	[−5]
3-T	2169	[+12]	2136	[−21]
16-T$_d$	2197	[+40]	2159	[+2]

[a] The deviation from experiment is given in brackets. CO stretching frequencies in the gas phase and in the zeolite are 2143 and 2157 cm^{-1}, respectively. [b] CCSD(T) calculations.

vibrations upon the adsorption on the Cu$^+$ ion show a red shift.[21,23] The blue shift of 30 cm^{-1} in the CO stretching frequency upon adsorption on Cu$^+$/MFI was found by Treesukol et al. using B3LYP together with small basis set and electrostatic embedding of 3-T model.[22] They concluded that the Madelung potential effect is responsible for the blue shift. This is in sharp contradiction to our results. Unfortunately, no CO frequency obtained with 3-T model used by Treesukol et al. without the Madelung potential effect was reported. Below we attempt to rationalize the performance of various models for description of vibrational dynamics.

The reliability and performance of various theoretical models can be analyzed on the basis of the systematic study of various effects presented above. In this analysis, we divide the approximations used into four groups: (i) the inner part (cluster) size effect, (ii) treatment of the long-range interactions, (iii) the approximations in the vibrational dynamics description, and (iv) the approximation in the electronic structure description. The experimental and calculated CO frequencies are compared in Table 4 for the gas-phase CO and for CO adsorbed on Cu$^+$/MFI. Experimental CO stretching frequency 2157 cm^{-1} does not necessarily correspond to the particular I2/T12 Cu$^+$ site in MFI used in Table 4. However, the use of a slightly different experimental value does not change the discussion presented below.

(i) Inner Part Size Effect. At the minimum energy structures, the oxygen atom of CO is relatively far from the framework oxygen atoms (always farther than 3.3 Å). However, the proper description of the CO interaction with the zeolite framework is important. When B3LYP description of this interaction (16-T$_d$ model, Table 4) is replaced with IPF description only (3-T model, Table 4), the CO stretching frequencies are improperly decreased by 28 and 23 cm^{-1} at the B3LYP and scaled CCSD(T) levels, respectively. Therefore, the use of sufficiently large cluster (or inner part within the combined scheme) is critical for correct description of the CO stretching dynamics. The minimum size of cluster (inner part) depends on the framework Al position and Cu$^+$ site. The geometry optimization with the inner part of the sizes used in this work (12−23 TO$_4$ tetrahedra) is computationally feasible at the RI−BLYP level, while it would be quite demanding at the B3LYP level. It is therefore important that the $\omega_{CO}-r_{CO}$ correlation is of the same accuracy at the B3LYP and BLYP levels. In fact, even other gradient-corrected density functionals are likely to perform well, for example, the PW91 functional was found to give satisfactory results. The termination of the framework Al atom also changes the CO stretching vibration; however, this change is relatively small. Changing the model definition from −Si−O−Al(OH)$_2$−O−Si− model (3-T and 9-T) to −Si−O−Al(OSi(OH)$_3$)$_2$−O−Si− (5-T$_d$ and 16-T$_d$ model), the CO stretching frequency increases by 1−4 cm^{-1} (Table 2). None of the previous computational studies of the CO interaction with Cu$^+$/zeolite system used sufficiently large cluster model for the description of CO stretching dynamics.

(ii) Treatment of Long-Range Interactions. Importance of the interactions beyond the inner part within the embedding scheme depends on the size of the inner part. These interactions are negligible (<1 cm^{-1}) for the inner part definition used in this study. The CO stretching frequency calculated with 16-T$_d$ model is the same with and without charges on atoms of CO (2188.0 and 2187.4 cm-$^{-1}$, respectively). We conclude that only the interaction of CO with surrounding framework atoms is important for correct description of the CO vibrational dynamics. Contrary to the conclusion of Treesukol et al., we state that the effect of the Madelung potential on the CO vibrational frequency is negligible.

(iii) Approximations in Vibrational Dynamics Description. The treatment of anharmonic effects for copper carbonyl species used in this study relies on the assumption that the CO vibration does not couple with vibrations beyond the heavy copper atom. This assumption justifies the use of the two-dimensional stretching model employed in this work. We found that for all X_n...Cu$^+$CO molecules the differences between the two-dimensional stretching and full-dimensional harmonic calculations are less than 0.5 cm^{-1}. The 2D stretching model works satisfactorily even for the Cu$^+$/MFI system. The error on the harmonic CO frequency for 1-T model ($Al(OH)_4^-$...Cu$^+$CO) is about 0.4 cm^{-1}. Another source of error is coupling with small amplitude motions of Cu$^+$/MFI which is not described properly at the harmonic level of theory. Two-dimensional anharmonic calculations (CO stretching + small amplitude vibration) for the I2/T12 site revealed that anharmonic contributions from low frequency vibrational modes are practically negligible (below 1 cm^{-1}). Thus, the largest anharmonic effect is the stretching−bending coupling with the Cu−C−O bending mode. The corresponding anharmonic correction for the gas-phase Cu$^+$CO ion at the CCSD(T) level is about 3 cm^{-1}. Since all important anharmonic effects are already included in vibrational calculations of the bare Cu$^+$CO ion, we consider the anharmonic correction of 29 cm^{-1} (CCSD(T)) as a reasonable estimate of the anharmonicity effect in the Cu$^+$/MFI system. Further improvements of this value should not differ more than 2 cm^{-1}. Proper description of the anharmonic effects is required when theoretical and experimental data are compared. However, the anharmonicity has only a minor effect on the shift of the CO stretching vibrations upon the adsorption in the Cu$^+$/ MFI system ($\Delta\nu_{CO}$ is −27 and −29 for $(CO)_g$ and CO/Cu$^+$/MFI, respectively).

(iv) Approximations in the Electronic Structure Description. For the discussion of the performance of methods used for the electronic structure description, it is important to compare data obtained with a sufficiently large model. On the basis of the 3-T model description of the zeolite environment (commonly used in the literature), one can conclude that B3LYP is predicting −23 cm^{-1} red shift in the CO stretching vibration upon the adsorption on Cu$^+$/MFI (Table 4), in qualitative disagreement with experiment. However, this disagreement is due to the small size of the model and not due to the exchange-correlation functional used. When sufficiently large cluster model is used, the B3LYP shows qualitatively correct +5 cm^{-1} blue shift. This is less than experimentally observed +14 cm^{-1} blue shift. The remaining discrepancy in B3LYP frequency is due to the nonconstant error in the CO vibrational frequency description at the B3LYP level. Better agreement with experiment was found at the scaled CCSD(T) level (+21 cm^{-1} blue shift).

The main advantage of the scaled CCSD(T) method is that in addition to correct relative energies of vibrational modes,

the absolute frequencies are also in excellent agreement with experimental data. IR band centered at 2157−2159 cm^{-1} was assigned to monocarbonyl of Cu^+/MFI. [9,11,12,15,20,59] The half-width of this band is about 10−20 cm^{-1}, depending on the temperature and pressure.[3,9,14] Thus, calculated CO stretching frequencies (2159−2170) falls well in the range of experimental data. Some authors deconvoluted this band into two peaks assigned to different Cu^+ sites (2151 and 2159 cm^{-1}).[4,9] Few attempts to correlate CO stretching frequencies with CO adsorption energies for Cu^+/MFI are also presented in the literature. Kumashiro et al. found that the CO stretching bands at 2159 and 2151 cm^{-1} correspond to higher and lower CO adsorption energies, respectively. On the contrary, Datka et al. found that the band at 2155 cm^{-1} corresponds to the Cu^+ sites with larger interaction energy with CO, while the bands at 2160 and 2165 cm^{-1} disappear upon heating of the sample.[60] The sites on the wall of the zigzag channel found in this work with slightly large CO stretching frequencies are the sites with small interaction energies with CO molecule.[23] While our results do not agree with the conclusions drawn by Kumashiro et al., they are in excellent agreement with the results obtained by Datka et al. Our model represents the high-silica MFI where the interaction of studied Cu^+CO with other Cu^+ or CO species is avoided. This model corresponds well with the samples used by Datka et al. (Si/Al ∼ 34, copper loading 20, 40, and 106%). On the contrary, Kumashiro et al. used samples with Si/Al ∼ 12 and high copper loading (147%). Using the sample with 106% copper loading, Datka et al. observed bands at 2143 and 2134 cm^{-1} in addition to bands at 2155, 2160, and 2165 cm^{-1}. They suggested that low energy bands are due to "oxygen containing Cu species".[60] Our results also suggest that low energy CO stretching bands are due to some other copper structures in zeolites than isolated Cu^+ ion in the vicinity of the single AlO_4 tetrahedron. The CO stretching band centered at 2157−2159 cm^{-1} was not deconvoluted in many other experimental studies.[3,11,13,61] For example, Zecchina et al. found that the band at 2151 cm^{-1} appears in the IR spectra together with the band at 2178 cm^{-1} and they concluded that these bands are due to the presence of dicarbonyl species.[61]

Our results also offer a possible interpretation of the fact that 2158 cm^{-1} band in the IR spectra of the CO/Cu^+/MFI system obtained in some laboratories can be deconvoluted into two bands while this deconvolution is not possible for spectra obtained in other laboratories. The Z6 sites on the wall of the zigzag channel are relatively stable sites for the Cu^+ ions.[50] If the framework Al distribution is favorable for population of these sites and the Cu^+ loading is low, the population of Z6 sites can be relatively high and CO IR band corresponding to these sites can be observed. On the contrary, if the framework Al distribution is statistical and the Cu^+ loading is high, the relative population of Z6 sites is low. Because of the small energy frequency difference between Z6 and other sites, the CO stretching band at 2158 cm^{-1} cannot be deconvoluted. Also, not only the Z6 sites but also the M6 sites on the wall of the main channel have smaller interaction energies with CO than sites on the channel intersection.

5. Conclusions

A novel scaling method based on the linear correlation between the CO bond length and CO stretching frequency has been proposed. Scaling was performed on a series of small models ($L-Cu^+CO$, L = H_2O, $(H_2O)_2$, OH^-, F^-, and $(F^-)_2$) and it was subsequently applied to the CO/Cu^+/MFI system. Computational advantage of the method stems from the fact that the description of the Cu^+CO ion interaction with its environment was reduced to calculation of the CO bond length changes at the DFT level of theory. The scaled CCSD(T) frequencies can be obtained with the same accuracy using both B3LYP and BLYP optimized CO bond lengths. Therefore, the large reduction of computational demands can be achieved using the resolution of identity approximation together with the BLYP exchange correlation functional.

The accuracy of the proposed method was checked by performing the analysis of all approximations included in our approach: the effect of anharmonicity, the effect of the cluster size used in the combined QM-Pot calculations, the effect of the unit cell size, and the effect of the Madelung potential. It was found that the CCSD(T) anharmonic correction for the gas-phase ion (29 cm^{-1}) is a reasonable estimate of the anharmonicity effect in the CO/Cu^+/MFI system (to within 2 cm^{-1}). The increase of the model size results in the increase of the CO stretching vibrations by more than 20 cm^{-1}, and therefore, large MFI models have to be used for accurate calculations of the site-specific CO stretching frequencies. The effect of the unit-cell size was marginal (−0.7 cm^{-1}). The effect of the Madelung potential on the CO frequency is rather small and can be neglected for large models (less than 1 cm^{-1}). We conclude that the CCSD(T)/DFT scaling provides essentially the same level of accuracy as obtained from the CCSD(T) calculations and the overall error should not exceed 5 cm^{-1}. It remains to be shown whether the same approach could be applied to other oxidation states of copper or to other metal cation carbonyl species.

Different definitions of the inner part used in the combined QM-pot description of the system were used for individual Cu^+ sites and framework Al atom positions. This deficiency of the model is probably quite small; however, it can be lifted by the use of a full-periodic DFT model. The work in this direction is starting in our laboratory.

An excellent agreement between the calculated and experimental CO stretching frequencies in the CO/Cu^+/MFI system was found. Calculated CO stretching frequencies are in the narrow range of 2159−2164 cm^{-1} for the Cu^+ sites on the channel intersection or on the wall of the main channel (experimental band centered at 2157−2159 cm^{-1}). Somewhat larger frequencies (3−6 cm^{-1}) were found for the Cu^+ sites on the wall of the zigzag channel. A blue shift of 21 cm^{-1} in the CO stretching frequency upon the adsorption on Cu^+/MFI was found at the scaled CCSD(T) level, in very good agreement with experimental shift of 14 cm^{-1}.

Acknowledgment. This work was supported by the grant form Ministry of Education of the Czech Republic (Project No. LN00A032, Center for Complex Molecular Systems and Biomolecules). Thanks go also to Joachim Sauer and Marek Sierka for providing QM-Pot program and to Julian Gale for providing GULP program.

References and Notes

(1) Lupinetti, A. J.; Strauss, S. H.; Frenking, G. Nonclassical metal carbonyls. In *Progress in Inorganic Chemistry*; 2001; Vol. 49, p 1.

(2) Zhou, M. F.; Andrews, L.; Bauschlicher, C. W. *Chem. Rev.* **2001**, *101*, 1931.

(3) Lamberti, C.; Bordiga, S.; Salvalaggio, M.; Spoto, G.; Zecchina, A.; Geobaldo, F.; Vlaic, G.; Bellatreccia, M. *J. Phys. Chem. B* **1997**, *101*, 344.

(4) Kumashiro, P.; Kuroda, Y.; Nagao, M. *J. Phys. Chem. B* **1999**, *103*, 89.

(5) Palomino, G. T.; Bordiga, S.; Zecchina, A.; Marra, G. L.; Lamberti, C. *J. Phys. Chem. B* **2000**, *104*, 8641.

(6) Bordiga, S.; Paze, C.; Berlier, G.; Scarano, D.; Spoto, G.; Zecchina, A.; Lamberti, C. *Catal. Today* **2001**, *70*, 91.
(7) Lamberti, C.; Palomino, G. T.; Bordiga, S.; Berlier, G.; D'Acapito, F.; Zecchina, A. *Angew. Chem., Int. Ed.* **2000**, *39*, 2138.
(8) Bolis, V.; Maggiorini, S.; Meda, L.; D'Acapito, F.; Palomino, G. T.; Bordiga, S.; Lamberti, C. *J. Chem. Phys.* **2000**, *113*, 9248.
(9) Kuroda, Y.; Yoshikawa, Y.; Kumashiro, R.; Nagao, M. *J. Phys. Chem. B* **1997**, *101*, 6497.
(10) Kuroda, Y.; Kumashiro, R.; Itadani, A.; Nagao, M.; Kobayashi, H. *Phys. Chem. Chem. Phys.* **2001**, *3*, 1383.
(11) Chen, H. Y.; Chen, L.; Lin, J.; Tan, K. L.; Li, J. *Inorg. Chem.* **1997**, *36*, 1417.
(12) Szanyi, J.; Paffett, M. T. *Catal. Lett.* **1997**, *43*, 37.
(13) Milushev, A.; Hadjiivanov, K. *Phys. Chem. Chem. Phys.* **2001**, *3*, 5337.
(14) Hadjiivanov, K.; Knozinger, H. *J. Catal.* **2000**, *191*, 480.
(15) Hadjiivanov, K. I.; Kantcheva, M. M.; Klissurski, D. G. *J. Chem. Soc., Faraday Trans.* **1996**, *92*, 4595.
(16) Bulanek, R.; Wichterlova, B.; Sobalik, Z.; Tichy, J. *Appl. Catal., B* **2001**, *31*, 13.
(17) Goldman, A. S.; Krogh-Jespersen, K. *J. Am. Chem. Soc.* **1996**, *118*, 12159.
(18) Bridgeman, A. J. *Inorg. Chim. Acta* **2001**, *321*, 27.
(19) Iwamoto, M.; Furukawa, H.; Mine, Y.; Uemura, F.; Mikuriya, S.; Kagawa, S. *J. Chem. Soc., Chem. Commun.* **1986**, 1272.
(20) Iwamoto, M.; Hoshino, Y. *Inorg. Chem.* **1996**, *35*, 6918.
(21) Ramprasad, R.; Schneider, W. F.; Hass, K. C.; Adams, J. B. *J. Phys. Chem. B* **1997**, *101*, 1940.
(22) Treesukol, P.; Limtrakul, J.; Truong, T. N. *J. Phys. Chem. B* **2001**, *105*, 2421.
(23) Davidova, M.; Nachtigallova, D.; Bulanek, R.; Nachtigall, P. *J. Phys. Chem. B* **2003**, *107*, 2327.
(24) Brand, H. V.; Redondo, A.; Hay, P. J. *J. Phys. Chem. B* **1997**, *101*, 7691.
(25) Broclawik, E.; Datka, J.; Gil, B.; Piskorz, W.; Kozyra, P. *Top. Catal.* **2000**, *11*, 335.
(26) Bludsky, O.; Silhan, M.; Nachtigall, P. *J. Chem. Phys.* **2002**, *117*, 9298.
(27) Pople, J. A.; Schlegel, H. B.; Krishnan, R.; Defrees, D. J.; Binkley, J. S.; Frisch, M. J.; Whiteside, R. A.; Hout, R. F.; Hehre, W. J. *Int. J. Quantum Chem. Symposia* **1981**, *15*, 269.
(28) Scott, A. P.; Radom, L. *J. Phys. Chem.* **1996**, *100*, 16502.
(29) Hout, R. F.; Levi, B. A.; Hehre, W. J. *J. Comput. Chem.* **1982**, *3*, 234.
(30) Cizek, J. *Adv. Chem. Phys.* **1969**, *14*, 35.
(31) Purvis, G. D.; Bartlett, R. J. *J. Chem. Phys.* **1982**, *76*, 1910.
(32) Becke, A. D. *Phys. Rev. A* **1988**, *38*, 3098.
(33) Becke, A. D. *J. Chem. Phys.* **1993**, *98*, 1372.
(34) Lee, C.; Yang, W.; Parr, R. G. *Phys. Rev. B: Condens. Matter* **1988**, *37*, 785.
(35) Devlin, F. J.; Finley, J. W.; Stephens, P. J.; Frisch, M. J. *J. Phys. Chem.* **1995**, *99*, 16883.
(36) Dolg, M.; Wedig, U.; Stoll, H.; Preuss, H. *J. Chem. Phys.* **1987**, *86*, 866.
(37) Antes, I.; Dapprich, S.; Frenking, G.; Schwerdtfeger, P. *Inorg. Chem.* **1996**, *35*, 2089.
(38) Frisch, M. J.; Pople, J. A.; Binkley, J. S. *J. Chem. Phys.* **1984**, *80*, 3265.
(39) Dunning, T. H. *J. Chem. Phys.* **1989**, *90*, 1007.
(40) Woon, D. E.; Dunning, T. H. *J. Chem. Phys.* **1993**, *98*, 1358.
(41) Schafer, A.; Horn, H.; Ahlrichs, R. *J. Chem. Phys.* **1992**, *97*, 2571.
(42) Rodriguez-Santiago, L.; Sierka, M.; Branchadell, V.; Sodupe, M.; Sauer, J. *J. Am. Chem. Soc.* **1998**, *120*, 1545.
(43) Sierka, M.; Sauer, J. *J. Chem. Phys.* **2000**, *112*, 6983.
(44) Treutler, O.; Ahlrichs, R. *J. Chem. Phys.* **1995**, *102*, 346.
(45) Feyereisen, M.; Fitzgerald, G.; Komornicki, A. *Chem. Phys. Lett.* **1993**, *208*, 359.
(46) Eichkorn, K.; Weigend, F.; Treutler, O.; Ahlrichs, R. *Theor. Chem. Acc.* **1997**, *97*, 119.
(47) Eichkorn, K.; Treutler, O.; Ohm, H.; Haser, M.; Ahlrichs, R. *Chem. Phys. Lett.* **1995**, *242*, 652.
(48) Eichkorn, K.; Treutler, O.; Ohm, H.; Haser, M.; Ahlrichs, R. *Chem. Phys. Lett.* **1995**, *240*, 283.
(49) Sierka, M.; Sauer, J. *Faraday Discuss.* **1997**, 41.
(50) Nachtigallova, D.; Nachtigall, P.; Sierka, M.; Sauer, J. *Phys. Chem. Chem. Phys.* **1999**, *1*, 2019.
(51) Gale, J. D. *J. Chem. Soc., Faraday Trans.* **1997**, *93*, 629.
(52) Molpro is a package of ab initio programs written by Amos, R. D.; Bernhardsson, A.; Berning, A.; Celani, P.; L. Cooper, D.; Deegan, M. J. O.; Dobbyn, A. J.; Eckert, F.; Hampel, C.; Hetzer, G.; Knowles, P. J.; Korona, T.; Lindh, R.; Lloyd, A. W.; McNicholas, S. J.; Manby, F. R.; Meyer, W.; Mura, M. E.; Nicklass, A.; Palmieri, P.; Pitzer, R.; Rauhut, G.; Schütz, M.; Schumann, U.; Stoll, H.; Stone, A. J.; Tarroni, R.; Thorsteinsson, T.; Werner, H.-J.
(53) Lindh, R.; Ryu, U.; Liu, B. *J. Chem. Phys.* **1991**, *95*, 5889.
(54) Deegan, M. J. O.; Knowles, P. J. *Chem. Phys. Lett.* **1994**, *227*, 321.
(55) Koningsveld, H. v.; Jansen, J. C.; Bekkum, H. v. *Acta Crystallogr.* **1987**, *7*, 564.
(56) Silhan, M.; Nachtigall, P.; Bludsky, O. *Chem. Phys. Lett.* **2003**, *375*, 54.
(57) Nachtigall, P.; Nachtigallova, D.; Sauer, J. *J. Phys. Chem. B* **2000**, *104*, 1738.
(58) Shao, L. M.; Zhang, L. N.; Zhou, M. F.; Qin, Q. Z. *Organometallics* **2001**, *20*, 1137.
(59) Lamberti, C.; Salvalaggio, M.; Bordiga, S.; Geobaldo, F.; Spoto, G.; Zecchina, A.; Vlaic, G.; Bellatreccia, M. *J. Phys. IV* **1997**, *7*, 905.
(60) Datka, J.; Kozyra, P. *Stud. Surf. Sci. Catal.* **2002**, *142*, 445.
(61) Zecchina, A.; Bordiga, S.; Palomino, G. T.; Scarano, D.; Lamberti, C.; Salvalaggio, M. *J. Phys. Chem. B* **1999**, *103*, 3833.